Ultrasonic Flow Field Measurement of a Rotating Flow with Free Surface

Yuji Tasaka[1], Yuichi Murai[1] and Makoto Iima[2]
[1]Laboratory for Flow Control, Hokkaido University, Sapporo 060-8628, Japan
[2]Department of Mathematical and File Science, Graduate School of Science, Hiroshima University, Hiroshima 739-8526, Japan

We developed a measurement technique to achieve the both of the interface detection and the flow field measurement simultaneously using UVP. The technique was adopted to investigate a temporally irregular surface switching of rotating fluids to clarify the mechanism of the phenomenon. Interface detection and estimation of two-dimensional velocity field from spatio-temporal velocity distributions successfully represented the development of the surface switching; change of the surface shape from circle to bow-tie shape via ellipsoid, and corresponding flow circulations on the velocity vector field.

Keywords: Flow field, Free surface, Rotating flow, Ultrasonic echo intensity

1 INTRODUCTION

Flow field measurement around largely deformed free surface has been desired in many research and development scenes, for instance in fundamental fluid physics, chemical engineering and civil engineering, etc. Traditional measurement tools, however, cannot provide detailed information about the both of the surface position and the flow field. Image-processing-based velocimetry such as PIV achieves that with high accuracy but has difficulties on industrial use because of limitations on the setup. In contrast with this UVP has some advantages for industrial use: UVP does not require transparency for fluids and walls of test sections; a non-invasive technique, spatio-temporal velocity measurement, etc. Recently, some works to enrich the measurable information on the UVP measurements have performed. There exist ultrasonic displacement meters and it is possible to add this function of the interface detection into UVP. We perform the interface detection on the results of UVP measurement, i.e. ultrasonic echo information and spatio-temporal velocity distribution [1].

Flows accompanied by a largely deformed free surface are one of the interesting problems in the fluid mechanics. Those motions are difficult to be analyzed and predicted by numerical analyses and theoretical ways. Good experimental works sometime provide a breakthrough to overcome difficulties to clarify the complex phenomenon. Here we utilize the developed technique to investigate recently discussed phenomenon, temporally irregular surface switching of rotating fluids [2,3]. The surface shape and the flow field around the deformed free surface in the surface switching are determined by UVP, and the development of the surface switching is represented.

2 IRREGULAR SURFACE SWITCHING OF ROTATING FLUIDS

Typical sequence of the surface switching of rotating fluids is shown in Fig. 1, where the top schema represents the top view of the surface shape with contours of surface height, and bottom photos are side view of the surface extracted from a movie. The process is summarized as follows: At the beginning of the process, (a)-(b) in the figure, a symmetry breaking of the free surface occurs, and the shape of the surface in the horizontal cross-section changes from an axisymmetric state to a line-symmetric state, elliptic in this step; then the line-symmetric surface has two humps at the bottom of the surface in the development of the deformation ((b)-(c)); after that the surface detaches from the disk ((d)); the detached free surface starts vertical oscillations and takes irregularly the axisymmetric state again; the axisymmetric surface sometime reattaches to the disk ((a)), but usually takes the symmetry breaking before that. Previous works clarified that the surface switching accompanies laminar-turbulent flow transition, namely the flow state for the axisymmetric surface is laminar and the turbulent for the line-symmetric surface. Reason of the elevation of the free surface in the surface switching may be a change of the pressure balance in the radial direction due to the turbulent flow mixing; turbulence transfers faster fluids near the lateral wall into the central part and vice versa.

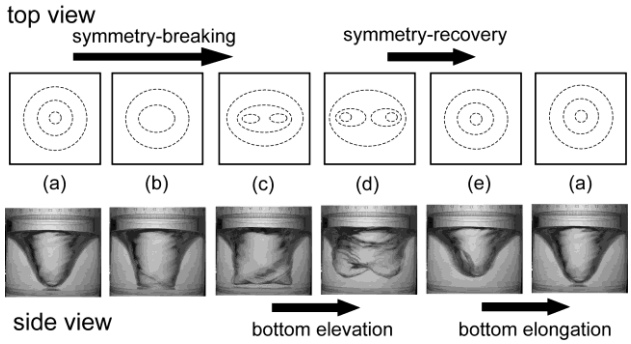

Figure 1: Typical sequence of the switching process; (top) illustrations for the top view of the free surface (bottom) side view of the free surface [3]

3 EXPERIMENTAL SETUP AND INTERFACE DETECTION

3.1 Experimental setup

Schema of the experimental setup for the interface detection and the flow field measurement is shown in Fig. 2(a). A cylindrical open vessel made of acrylic resin with $R = 42$ mm in radius has a glass disk as its bottom. There is a certain lateral clearance, $\Delta R = 0.3$ mm, between the cylinder and the disk. Tap water is used as the test fluid and the depth of the water layer in the vessel is $H = 40$ mm at rest; the corresponding aspect ratio becomes $\Gamma = H/R = 0.95$. The bottom disk is rotated by a motor with a constant speed of rotation, $\Omega = 13.2$ Hz. For this value, the Reynolds number, $Re = 2\pi\Omega R/\nu$ (ν is kinematic viscosity of water), is 1.46×10^5.

UVP was utilized to obtain spatio-temporal velocity profiles and ultrasonic echo information. An ultrasonic transducer (TDX) with 4 MHz in the resonance frequency was mounted on the side wall of the cylinder with 8 mm in height from the disk. The TDX faced the center of the cylinder and the UVP measured time variation of the radial velocity component along the radial direction, i.e. $u_r(r, t)$. UVP monitor model Duo recorded and processed ultrasonic echo information. Time and space resolutions of the measurement are 13 ms and 0.74 mm. Particles of porous resin (50-60 μm in diameter and 1020 kg/m^3 in density) were seeded into the water as the flow tracers for the UVP measurement.

A halogen ramp illuminated fluid layer from the side, and the back-lighting images of the free surface were recorded by a digital video camera with 29.97 fps. Samples of the obtained images are shown in Fig. 2(b), where the black lines in the figure indicate measurement line of the UVP.

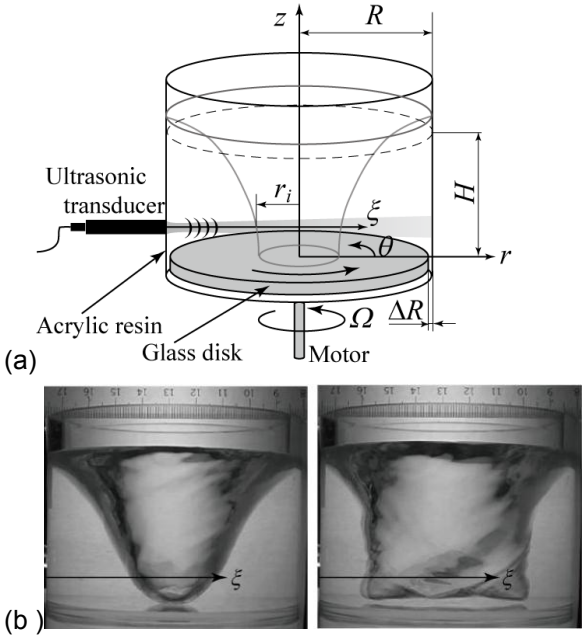

Figure 2: (a) Schema of experimental setup and (b) examples of surface shape

3.2 Interface detection

To achieve the interface detection together with the velocity field measurement, two methods, Doppler method and echo intensity method, are utilized. These have different disadvantages on the interface detection and thus are used in a complementary style. Figure 3(a) shows original, spatio-temporal velocity distribution in the development of the symmetry breaking, corresponding to (a)-(b)-(c)-(d) in Fig. 1, measured by UVP. The symmetry breaking of the rotating free surface provides periodic variation of the velocity, and the magnitude of the variation increases with time. With the development, discontinuous lines appear in the radial direction because of reflection of ultrasonic wave at the interface. Sovel filter, a kind of differential filter, enhances the 'discontinuous edge' as shown in Fig. 3(b), and we can detect interface position by finding the edges. This method, however, does not work at which the flow direction greatly changes, local minimal or maximal pints on the variation of the interface position in this case. On the other hand, the ultrasonic echo intensity indicates higher values only at the extremal points as shown in Fig. 3(c). It is because the inclination angle of the surface is much larger than the divergence angle of the ultrasonic wave, 5 deg. in this case, without the extremal points on the variation of the surface position, and thus the ultrasonic transducer cannot receive the echo reflected at the interface.

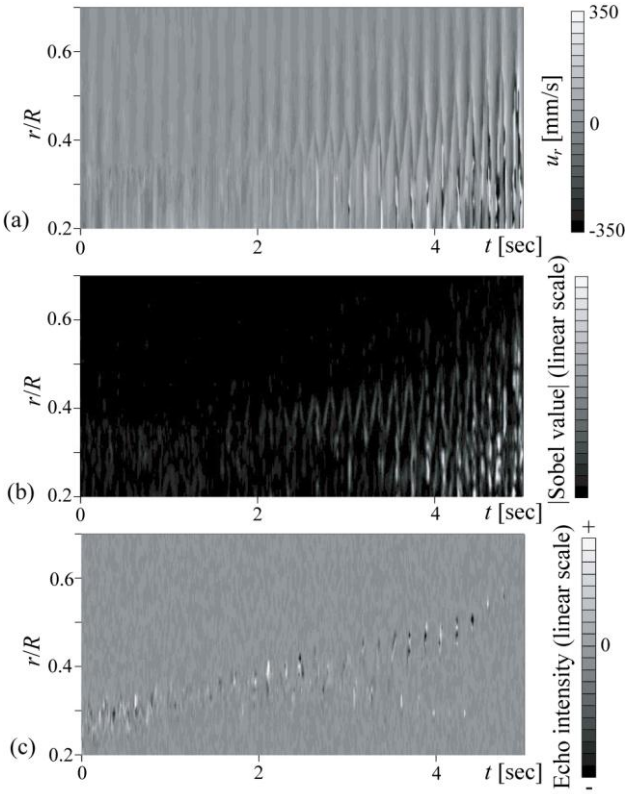

Figure 3: (a) Original velocity distribution, (b) Sovel-filtered value of the velocity, (c) variation of the corresponding ultrasonic echo information [1]

A variation of the free surface position in the radial direction, r_i, detected by above two methods is shown in Fig. 4, where the surface height at the center of the vessel, h, determined from the movie simultaneously taken and the intensity of the spatial velocity fluctuation, $u_{r,\mathrm{rms}}$, are also shown. The black and gray lines in the figure indicate original data and moving-averaged one, respectively. There seems strong correlation between the development of the surface deformation and the increase of the velocity fluctuation. The variations represent process of the symmetry breaking and detachment of the free surface: The surface deformation due to the symmetry breaking proceeds increase of the velocity fluctuation that provides the flow mixing; when the fluctuation becomes large enough, the free surface detaches from the bottom; the surface deformation and the increase of the velocity fluctuation are further enhanced.

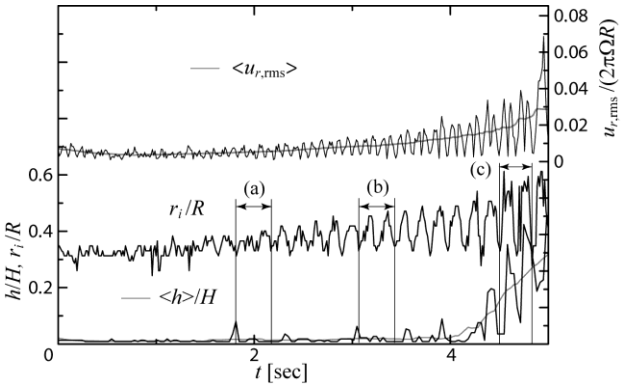

Figure 4: Variations of the surface height, h, radial position of the interface, r_i, and the intensity of the velocity fluctuation, $u_{r,\mathrm{rms}}$, where the black and gray lines represent original data and moving-averaged one

4 RESULTS AND DISCUSSIONS

4.1 Surface shape

According to the observation of the free surface shape in the sequence of the surface switching (see Fig. 1), surface shape on the horizontal cross-section changes from circle to ellipsoid. It is, therefore, reasonable to assume that two cycles of the variation on r_i shown in Fig. 4 corresponds to the whole periphery of the free surface; namely the local minimal and maximal positions on r_i correspond to the miner and major axes of the ellipsoidal free surface. By giving period of the rotation T, $r_i(t)$ can be converted into $r_i(\theta)$, where the T is not constant and changes with respect to the surface deformation. Figure 5 shows the result of the conversion, i.e. estimated surface shape expressed in the polar coordinates, where the diagonal crosses represent the obtained surface position in the radial direction and the lines connecting these points are given by closed B-Spline interpolation. Here we also converted spatio-temporal distribution of the radial velocity component, $u_r(r, t)$ into $u_r(r, \theta)$ in the same way of the conversion from $r_i(t)$ to $r_i(\theta)$ by applying Taylor's frozen hypothesis that assumes the local flow structure doesn't change against the advection.

Three circular distributions in the Fig. 5 represent the surface shape and the radial velocity distribution at the beginning of the symmetry breaking (a), the adjacent (b) and immediate (c) states for the detachment of the free surface from the rotating disk. Corresponding time series of r_i, the surface height h and the velocity fluctuation $u_{r,\mathrm{rms}}$ for these states are indicated in Fig. 4. In Fig. 5(a) the surface deformation is small and its shape is still circular. The radial velocity due to the surface deformation is also small. In the adjacent state for the surface detachment from the disk, Fig. 5(b), the surface largely deforms and its shape becomes ellipsoid. The radial velocity is enhanced and the flow direction changes around the minor and major axes

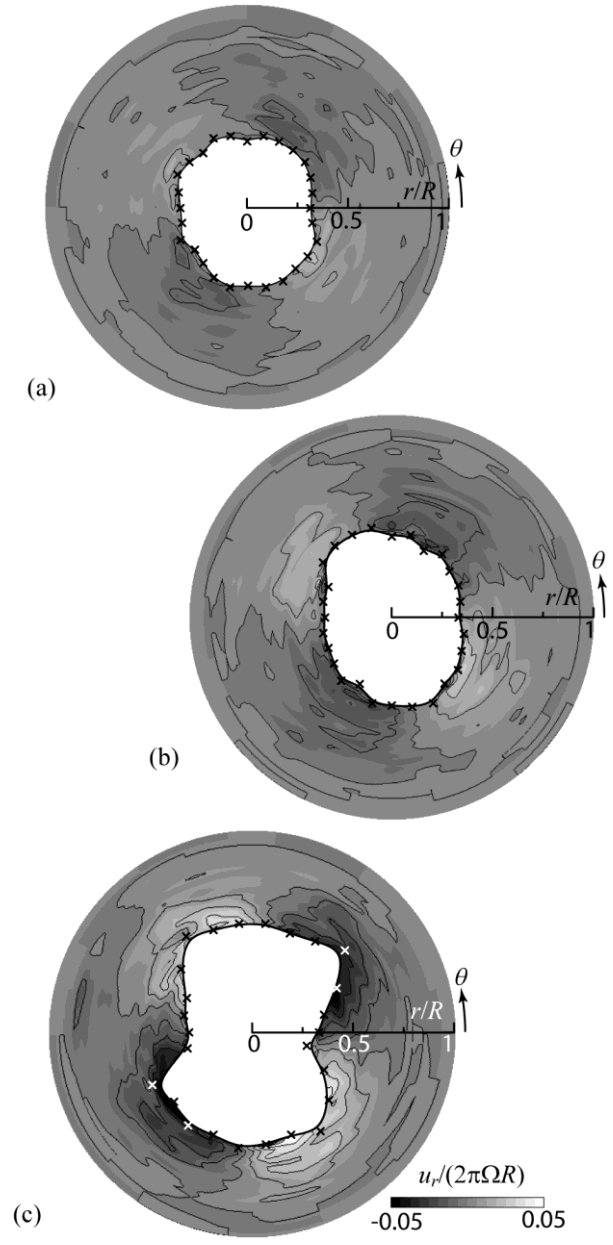

Figure 5: Estimated surface shapes $r_i(\theta)$ and distribution of the radial velocity component $u_r(r,\theta)$ in polar coordinates; original data for figs are indicated in Fig. 4.

points. After the free surface detaches from the bottom, surface deformation is further developed and the shape is no longer ellipsoid: Smaller curvature sides of the ellipsoid are concaved and four apexes appear like a bow tie. The flow seems to be pushed out by two facing apexes.

4.2 Estimation and evaluation of the flow field

To evaluate the flow field around the free surface that deforms with time, we estimate the distribution of the tangential velocity component u_θ from $u_r(r, \theta)$ and form the two dimensional velocity vector field. By assuming that the axial velocity is small enough in comparison with u_r and u_θ, u_θ is derived from the two-dimensional equation of continuity in the polar coordinate as

$$u_\theta(r,\theta) = u_\theta(r,0) - \int_0^{2\pi} \frac{\partial}{\partial r}(ru_r)d\theta \qquad (1)$$

Here giving $u_\theta(r, 0)$ to above equation is impossible on the present data set. But using the whole circumference average of $u_\theta(r, \theta)$,

$$\begin{aligned} u'_\theta(r,\theta) &= u_\theta(r,\theta) - \langle u_\theta \rangle_\theta (r) \\ &= \frac{1}{2\pi}\int_0^{2\pi}\int_0^{\phi}\frac{\partial}{\partial r}(ru_r)d\theta d\phi - \int_0^{\theta}\frac{\partial}{\partial r}(ru_r)d\theta, \end{aligned} \qquad (2)$$

where the brackets, $<>_\theta$, mean the whole circumference average. To prevent noise amplification due to the numerical difference, median filtering with 3 times 3 lattice size has been applied on the original data of $u_r(r, \theta)$ before the estimation. The trapezium scheme is used for numerical integration.

Figure 6 shows the results of the estimation; (a) at the beginning of the symmetry breaking, (b) at the immediate state of the surface detachment. Corresponding radial velocity distributions for these figures are (a) and (c) in Fig. 5. As expected in the radial velocity distribution, variation on the velocity field around the circular free surface is extremely small (Fig. 6(a)). It means the flow field is axisymmetric. On the other hand for the largely deformed free surface, there exists a typical flow structure due to surface deformation, even though the error vectors appear near the deformed, bow-tie-shaped free surface (Fig. 6(b)). Four large circulations are formed around the apexes of the surface, and these circulations may modify the pressure distribution and provide the strange surface shape at the bottom as shown in Fig. 2(b).

5 CONCLUSION

We developed a non-invasive technique to measure the both of the surface shape and the flow field around the free surface by utilizing UVP. The technique was applied to determine the behavior of the free surface and the surrounding fluid motion in the temporally irregular surface switching of a rotating fluid. Doppler method that utilizes characteristic velocity variation around the free surface on the results of the UVP measurements, and echo intensity method were employed to detect the free surface position. These methods act to redeem their disadvantages each other. Obtained results represent the development of the free surface and corresponding flow field as well; the free surface deformation from circle to bow-tie shape via ellipsoid. Velocity vector fields estimated from the radial velocity component with applying Taylor's frozen hypothesis show four local circulation of the flow for the bow-tie shaped surface.

ACKNOWLEDGEMENT

This study is partially supported by Core Research for Evolutional Science and Technology (CREST) No. PJ74100011.

REFERENCES

[1] Murai Y, *et al*.: Ultrasonic detection of moving interfaces in gas-liquid two-phase flow, Flow Meas. & Inst. 21(2010), 356-366.
[2] Suzuki T, Iima M, Hayase Y: Surface switching of rotating fluid in a cylinder, Phys. Fluids 18(2006), 101701.
[3] Tasaka Y and Iima M: Flow transition in the surface switching of rotating fluid, J. Fluid Mech. 636(2009), 475-484.

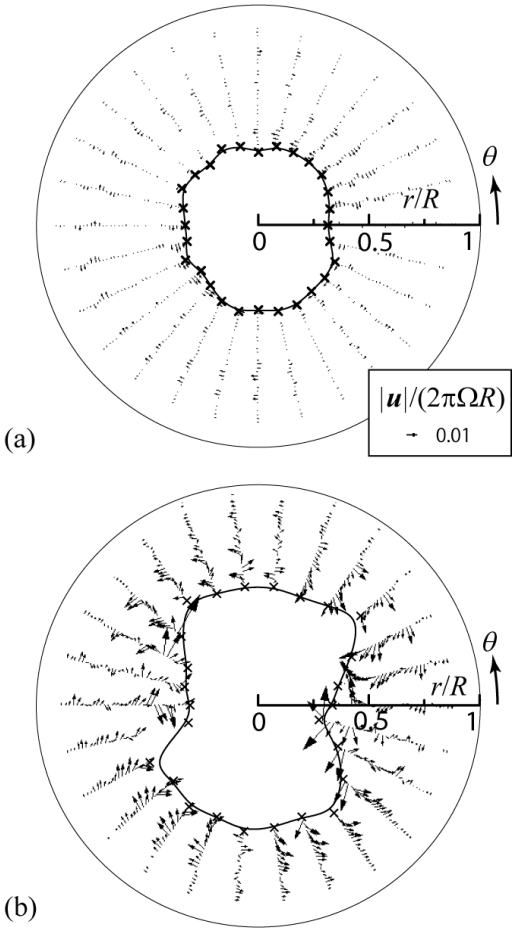

Figure 6: Estimated velocity vector field around the rotating free surface; corresponding radial velocity distributions are shown in Fig. 5(a) and (c)